Parallel Excitation: Making SENSE of High-Field Body MRI

Yudong Zhu, Ph.D
GE Global Research, Niskayuna, NY, USA

MR imaging at high B0 field strength presents significant diagnostic opportunities derived from enhancements in SNR, spectral resolution and image contrast. However there are technical challenges that substantially hamper the practice of high-field MRI, including a major one that is related to the exploitation of the radio frequency EM field (B1 field and concomitant E field). As field strength increases, the degradation in B1 homogeneity due to increased wave behavior and source-subject interaction (1-5) may result in compromises in image uniformity or contrast fidelity, and the exacerbation in RF power deposition (SAR) at an increasing rate (2,6) may pose considerable constraints on the use of RF pulses or volume transmit coils. Both the B1 inhomogeneity and SAR problems become more prominent with an increase in object size. While *in vivo* head imaging has been robustly demonstrated at a B0 field strength of 7 Tesla or even higher (6,7), the lack of effective measures managing both the B1 inhomogeneity and SAR problems appears to be holding up the extension of the head imaging success to body imaging. This talk introduces promising solutions provided by parallel excitation, an emerging technology that is based on orchestrated RF transmit with a distributed array of coils, as opposed to the convention of single-channel transmit with a volume coil.

Parallel Excitation Overview

At the 2002 ISMRM meeting, Zhu (8), and independently Katscher et. al. (9,10), introduced, as a means to speed-up 2D or 3D RF pulses and facilitate reduced-FOV imaging, a multi-channel RF transmit architecture and a first version of the parallel excitation concept – transmit-SENSE. With the new approach, parallel RF transmit orchestrates B_1 variation by driving distributed transmit coils with parallel RF pulses (Fig. 1), where calculation of the parallel pulses relies on such inputs as the desired excitation profile and the individual coils' B1 field patterns. A continuing study (11,12) elucidated parallel excitation's two fundamental characteristics: the spatiotemporal modulation of B1 field and increased degrees of freedom of RF transmit. The same study further extended the transmit-SENSE idea, and presented parallel excitation as a means to accelerate the creation of a general excitation profile (including a uniform one) and to manage RF power deposition in the meantime. To a great extent, parallel excitation, as it is known now, represents a RF-transmit counterpart to such RF-receive technology as phased array (13) and SENSE/SMASH (14,15) — a high degree of symmetry exists not only between the transmit goal of managing the speed/SAR of transverse-magnetization induction and the receive goal of managing the speed/SNR of transverse-magnetization mapping, but also between the means to achieve the respective goals.

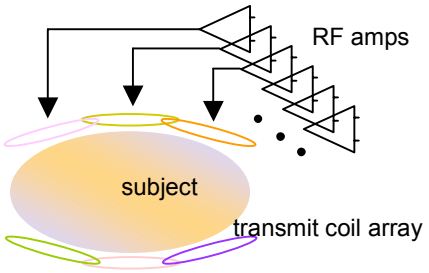

Fig. 1 With parallel excitation, simultaneous driving of a distributed array of transmit coils with parallel RF pulses orchestrates B_1 spatiotemporal variation. The calculation of the parallel pulses relies on such inputs as the desired excitation profile and individual coils' B1 field patterns.

It is to be noted that a majority of the existing assessments of the B1 inhomogeneity and SAR issues were made against the canonical RF transmit setup, which involves pulsing a volume coil (16,17) to induce a B_1 field that is temporally modulated yet, ideally, spatially homogeneous. Carrying out 1D-selective or non-selective excitation with this canonical setup is a most common

practice in MR imaging. From a flip-angle/image-contrast perspective, the excitation profile over the non-selected spatial dimensions typically tracks the B1 field profile over the same dimensions. The profile is thus subject to significant distortion when B1 inevitably degrades in uniformity at high B0 field strength. Multi-dimensional excitation has some potential to compensate for the excitation profile distortion, yet is not considered a practical solution because of its pulse width and/or excessive demand on gradient capability. From a SAR perspective, RF power dissipation within the subject is proportional to the product of tissue conductivity and the square of radio-frequency E field strength. Granted, a radio-frequency B1 field in the subject is always accompanied by a concomitant E field and hence RF power dissipation, yet the canonical setup is at best not very conducive to efficient SAR management. The very practice of striving for B1 homogeneity over a substantial volume (in establishing the canonical transmit setup) tends to cause the concomitant E field to extend broadly and to leave duty cycle reduction (e.g., re-shaping RF pulse or stretching TR) as the sole avenue for containing SAR. The lack of SAR efficiency manifests in planar imaging for example, where a simple adjustment in location/thickness of slice prescription typically has little impact on the RF power dissipation. For curbing the prohibitive B0 strength- and object size-dependent SAR increase, one would hope that the volume coil approach could somehow make the best of a situation where the imaged region is only a small fraction of the subject volume covered by the coil.

In sharp contrast to the volume coil approach, parallel excitation orchestrates spatial as well as temporal B1 variation by driving an array of distributed transmit coils with parallel RF pulses. The new approach enables up to N-fold (N = the total number of transmit coils) acceleration of multi-dimensional excitation pulses without adding strains to gradients (11). This promises unprecedented capacity for creating excitation profiles and, when applied to address the B1 inhomogeneity issue at high B0 strength in particular, for creating a uniform flip angle profile over a slice or a volume. To ensure flip-angle/image-contrast fidelity, rather than critically relying on B1 homogeneity, the new approach calibrates B1 field profiles associated with the multiple transmit coils, and uses the results to calculate pulses and control 2D or 3D excitation profiles (18). The departure from the canonical practice of striving for B1 homogeneity further provides parallel excitation with a unique leverage to ameliorate the SAR issue. Intuitively, when the imaged region is a fraction of the subject volume covered by the transmit coils, optimized use of the coils such that, for example, coils near the imaged region contribute more than the rest, may avoid unnecessarily high RF power dissipation. Prior studies formulated the pulse design problem as a constrained optimization and demonstrated that the extra degrees of freedom inherent in a parallel transmit system can be advantageously exploited to tailor the E field and reduce SAR (11,12). For the small-tip-angle regime or its large-tip-angle extension (19) in particular, the pulse design method assumes the form of minimizing a quadratic function subject to linear constraints, where the constraints capture what is required of the RF pulse waveforms for creating the desired profile and the quadratic function relates the RF pulse waveforms to RF power dissipation. A slightly adapted version of this constrained optimization formulation (20) is used in the examples given in the next two sections, which illustrate in some detail parallel excitation pulse designs that minimize RF power dissipation while creating desired excitation profiles.

B1 Imhomogeneity Effect and Its Correction

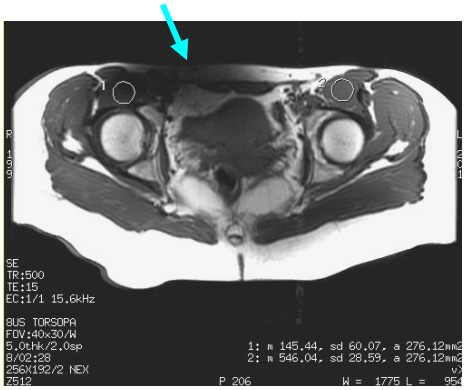

Fig. 2 Body imaging at 3T with volume coil transmit: the very noticeable shading over the FOV was primarily caused by the degradation in B1 homogeneity.

At high frequencies, increased wave behavior and source-subject interaction pose a great challenge to volume coil-based excitation profile control. Despite efforts to improve B1 uniformity (e.g., by following the classic approach of quadrature-drive birdcage coil (16,1)), the B1 field present in the subject is generally affected by complex eddy currents and displacement currents. These induced currents could significantly modify a volume coil's ideal field pattern, causing flip-angle/image-contrast variation over the field-of-view. Fig. 2 illustrates the issue in a 3T body imaging study, where B1 inhomogeneity led to significant flip-angle nonuniformity over the field-of-view. At even higher field strength, a head-imaging study conducted on a 7T system for example, reported >40% variations in B_1 magnitude and considerable resulting image inhomogeneity (6). While quantitative prediction of B1 field requires solving Maxwell's equation, a qualitative way to track one of the high-frequency effects is to note the EM field wavelength in the subject, which is roughly proportional to the inverse of the product of the B0 field strength and the square root of tissue dielectric constant. At a wavelength on the order of 20cm in a human subject at 3T, and about a factor of two shorter at 7T, some modulation of B1 field in line with a standing wave pattern can occur in both head and body imaging, giving rise to a conspicuous flip-angle nonuniformity artifact sometimes referred to as dielectric resonance (21,22).

Use of parallel excitation to address the effect of B1 inhomogeneity is illustrated below with simulations. A case involving an 8-element transmit coil array is examined in particular (Fig. 3). The transmit array is composed of eight surface coils, which are driven in parallel under the control of eight parallel transmit channels. A canonical RF transmit case involving a 16-rung birdcage coil is also examined for comparison purposes. The birdcage coil is of the same overall size (Fig. 3) and is driven in quadrature under the control of a single transmit channel. In both cases the imaged object is a concentrically located long cylinder, with a diameter of 40cm, and permittivity and conductivity comparable to that of human tissue (23).

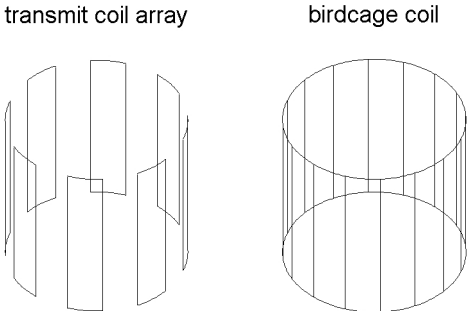

Fig. 3 The 8-element transmit coil array (left) is composed of eight elongated surface coils azimuthally distributed on a ∅44cm shell, each with a length of 42cm and an angular aperture of 22.5°. The 16-rung birdcage coil (right) is of the same overall size.

In the birdcage coil case, both the B1 and E fields corresponding to the standard quadrature-drive mode were quantified. Excitation profiles resulting from a non-selective or slice-selective excitation was further simulated. Fig. 4a-b show for the B0 strength of 3T and 7T, respectively, the profiles as a function of (x,y) over a center axial slice of the cylinder object. As a reference, the same simulation was also carried out at a head-size imaging scale, with a smaller birdcage coil and a ∅24cm cylinder object (Fig. 4c-d). The effects of inhomogeneous B1 transmit field at high B0 strength are readily appreciated at both the body-size scale and the head-size scale. The effects at 7T appear to be more pronounced due to, in part, a reduced wavelength.

To a certain extent the effects of inhomogeneous B1 can be corrected for by additionally controlling spatial selectivity over the x-y dimensions, with a multi-dimensional selective

excitation that is designed based on a calibrated B1 field map. This single-channel selective excitation pulse design can be treated as a degenerate case (11) of parallel excitation pulse design. For simulating 2D selective excitation in 7T body imaging, the latest algorithm based on the constrained optimization formulation (20) was employed. The pulse calculation used as inputs the target (uniform) excitation profile, the B1 field map, as well as an echo-planar k_x-k_y trajectory consisting of 48 k_x=constant lines (views) with spacing Δ_{kx}=1/42 cycles/cm. Assuming robust play out of the long 2D pulse, the simulation yielded an excitation profile shown in Fig.4a. The echo-planar trajectory samples the k_x dimension more coarsely than the k_y dimension, yet, as part of the 2D profile control scheme, the ensuing 48 x-dimension spatial harmonic patterns appeared to provide an adequate amount of levers compensating for the B1 field inhomogeneity and achieving a

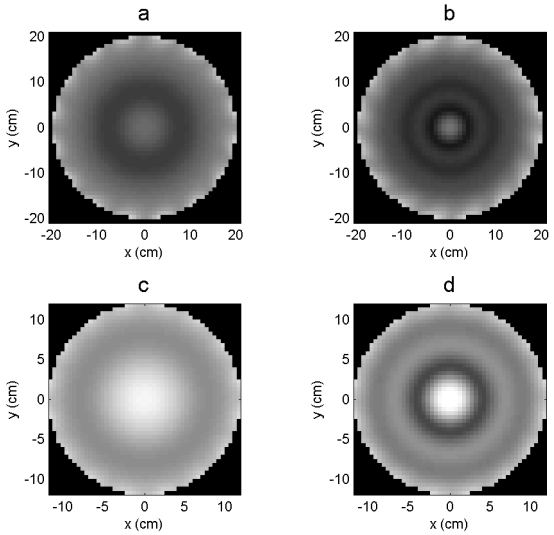

Fig. 3 Excitation profiles resulted from a non-selective or slice-selective excitation with a quadrature-drive birdcage coil. The effects of inhomogeneous B1 field present when imaging at the body-size scale at 3T (a) and 7T (b). The effects also present when imaging at the head-size scale at 3T (c) and 7T (d).

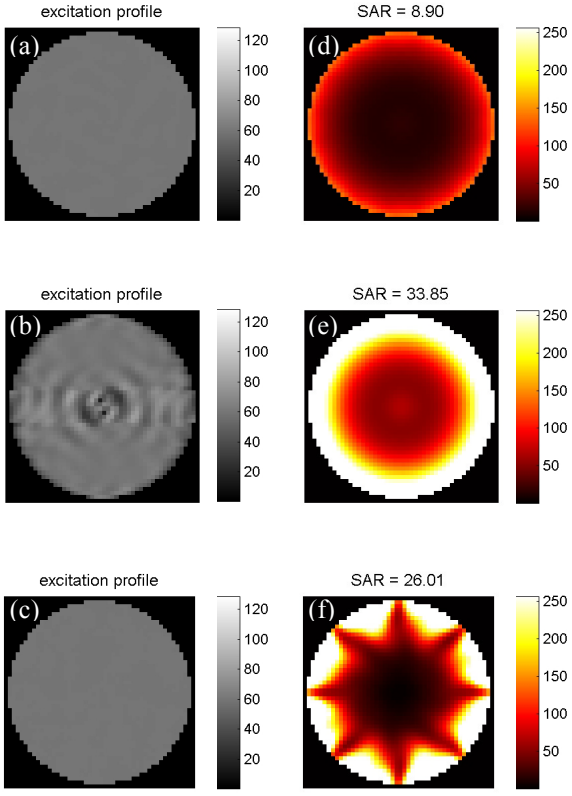

Fig. 4 2D excitation targeting a uniform excitation profile: profiles resulting from birdcage-coil transmit with a 48-view 2D pulse (a), birdcage-coil transmit with a 12-view 2D pulse (b) and parallel transmit with a 12-view 2D pulse (c); corresponding overall and spatially mapped RF power dissipation (d-f).

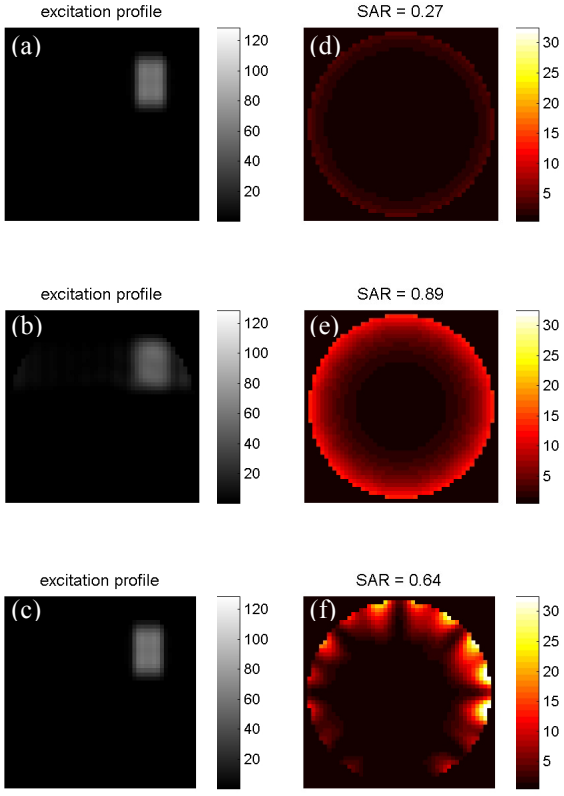

Fig. 5 2D excitation targeting a local-ROI excitation profile: profiles resulting from birdcage-coil transmit with a 48-view 2D pulse (a), birdcage-coil transmit with a 12-view 2D pulse (b) and parallel transmit with a 12-view 2D pulse (c); corresponding overall and spatially mapped RF power dissipation (d-f).

uniform excitation profile. This 2D pulse however, with a length exceeding 20 msec on a nominal clinical scanner, is hardly practical. Reducing the number of k_x=constant lines by a factor of 4 while maintaining Δ_{kx} improved the practicality of the 2D pulse. The reduction nevertheless led to an unsatisfactory result in terms of managing the B1 inhomogeneity effects (Fig. 4b).

In the transmit array case, solutions to Maxwell's equations (24) at various B0 field strengths were evaluated, and the B1 and E fields due to individual transmit coils were quantified. Again, for simulating 2D selective excitation in 7T body imaging, the latest algorithm based on the constrained optimization formulation (20) was employed. The parallel transmit architecture allowed up to a factor of 8 acceleration of multi-dimensional selective excitation compared to the birdcage coil approach. In one example, the parallel RF pulses were calculated based on an echo-planar k_x-k_y trajectory consisting of 12 k_x=constant lines with spacing Δ_{kx}=1/10.5 cycles/cm. This design represents a 4-fold acceleration, and the result obtained was satisfactory (Fig. 4c). For another design that represents a 6-fold acceleration, a comparable result in terms of reduction of B1 inhomogeneity effects was also obtained.

In addition to an excitation profile that is uniform over a large field-of-view, simulations were also conducted studying the creation of an excitation profile that is uniform over a selected region and zero elsewhere, which is of interest for imaging a local volume within a subject. The excitation pulses responsible for the results shown in Fig. 4a-c were recalculated, with a rectangular local ROI excitation profile replacing the original uniform profile. Fig. 5a-c show, respectively, the results with the birdcage 48-view 2D pulse, the birdcage 12-view 2D pulse and the transmit array 12-view 2D pulse. These results are counterparts to the uniform profile results of Fig. 4a-c. Again, the loss in effectiveness creating the desired profile is apparent with the birdcage 12-view 2D pulse – the truncation of higher frequency spatial harmonics resulted in a profile that is blurred (Fig. 5b). In comparison, the parallel transmit approach was able to not only accelerate the excitation but create the desired profile with good quality (Fig. 5c).

SAR Management

RF power dissipation in the subject due to RF transmit causes heating, which is a primary safety concern associated with the use of RF coils and excitation pulses. An elevated RF power deposition can result from an increase in flip angle, duty cycle, object size or main field strength. As discussed earlier, the canonical RF transmit setup involving the use of a volume transmit coil is associated with a rapid escalation in RF power dissipation as the main field strength increases. This for example has been a major cause to the significant reduction in the scope/scale of 3T imaging protocols compared to that of 1.5T – to conform to the FDA SAR guidelines, a number of imaging sequences that are routinely used on 1.5T clinical scanners must have their RF duty cycle lowered when ported for use on 3T scanners (e.g., with stretched TR's or alternative/re-shaped RF pulses, often at a cost to imaging speed / coverage / contrast). The impact of SAR limits is acutely felt when the main field-strength factor is compounded by the object-size factor. Although imaging with head coils have been demonstrated *in vivo* at 7T or even higher, imaging with body coils remain rare at field strengths above 3T. Issues with excessive SAR and RF power have practically limited the size of compatible conventional volume transmit coils, considerably hampering the development of body applications on high field scanners.

Parallel transmit appears to be associated with a relatively tamed curve relating RF power dissipation to B0 strength and object size, which offers opportunities to ameliorate the SAR issue in high-field imaging without forcing sacrifices in imaging sequence performance/choices. In a sense, parallel transmit's goal of maximizing flip-angle to RF-power ratio mirrors parallel receive's goal of maximizing signal to noise ratio — results from parallel receive research should provide valuable intuition in understanding and advancing the parallel transmit technology. While

it is well appreciated that with the canonical transmit approach RF power dissipation is correlated to the excitation profile shape, the correlation between the two takes on new dimensions with the parallel transmit approach. Both transmit array geometry and parallel pulse design impact the correlation in significant ways (20) and should be optimized to maximize SAR efficiency.

For the examples described in the previous section, we note here the performance of various excitation pulses from the RF power dissipation perspective. Fig.4d-f show the RF power dissipation as functions of (x,y) for, respectively, the birdcage 48-view 2D pulse, the birdcage 12-view 2D pulse and the transmit array 12-view 2D pulse. It should be pointed out that if one had time-condensed the birdcage 48-view 2D pulse by a factor of 4 with a set of faster gradients, the overall and the spatially mapped RF power dissipation would both have increased by a factor of 16 (due to a 4-fold increase in pulse amplitude required for maintaining the flip angle), leading to significantly worse RF power dissipation than that of the parallel transmit 2D pulse. For overcoming B1 inhomogeneity effects and creating the flat excitation profile, and for managing SAR in the meantime, the parallel transmit approach demonstrated great potential. Fig. 5d-f show the RF power dissipation for the three selective excitation approaches in the local ROI profile example. The parallel transmit approach again compared favorably with the other two. Moreover, this example suggested that more opportunities exist for SAR reduction in local ROI imaging. Such opportunities are expected to increase still with a full-fledged setup involving parallel transmit coils distributed in all three spatial dimensions.

Summary

Parallel excitation represents a new research area. In the context of high-field MRI, this talk focuses on illustrating parallel excitation's potential for managing SAR while creating desired excitation profiles, which has been a major challenge facing the conventional RF transmit approach. To help advance the practice of high-field imaging and to realize the full potential of parallel excitation, further research efforts are clearly needed, which include RF transmit system instrumentation, transmit array design/fabrication, B1 and RF power calibration, parallel excitation pulse design and imaging sequence/protocol development. The past several years have witnessed a fast-pace development of parallel excitation methodology. At the 2005 ISMRM meeting, a number of studies covering such subjects as B1 calibration, pulse design and hardware development were presented in various scientific sessions (25). One particularly encouraging progress reported at the meeting was the successful prototyping of two parallel transmit MR scanners (26,27), which promises to facilitate experimental investigations and accelerate continuing research.

Acknowledgements

I would like to thank Sonal Josan of the Electrical Engineering Department, Stanford University for her assistance in developing some of the numerical simulation code.

References

1. G.H. Glover, C.E. Hayes, N.J. Pelc, W.A. Edelstein, O.M. Mueller, H.R. Hart, C.J. Hardy, M. O'Donnell and W.D. Barber, Comparison of linear and circular polarization for magnetic resonance imaging, J Magn Reson, 64:255-270, 1985.
2. C.M. Collins, S. Li and M.B. Smith, SAR and B1 field distributions in a heterogeneous human head model within a birdcage coil, Magn Reson Med, 40:847-856, 1998.
3. T.S. Ibrahim, R. Lee, B.A. Baertlein, A.M. Abduljalil, H. Zhu and P.L. Robitaille, Effect of RF coil excitation on field inhomogeneity at ultra high fields: a field optimized TEM resonator, Magn Reson Imag, 19:1339-1347, 2001.
4. C.M. Collins and M.B. Smith, Signal-to-noise ratio and absorbed power as functions of main magnetic field strength, and definition of "90 degrees" RF pulse for the head in the birdcage coil, Magn Reson Med, 45:684-691, 2001.
5. B.L. Beck, K. Jenkins, J. Caserta, K. Padgett, J. Fitzsimmons and S.J. Blackband, Observation of significant signal voids in images of large biological samples at 11.1T, *Magn Reson Med*, 51:1103-1107, 2004.
6. J.T. Vaughan, M. Garwood, C.M. Collins, W. Liu, L. DelaBarre, G. Adriany, P. Andersen, H. Merkle, R. Soebel, M.B. Smith and K. Ugurbil, 7T vs. 4T RF power, homogeneity, and signal-to-noise comparison in head images, Magn Reson Med, 46:24-30, 2001.
7. R.E. Burgess, Y. Yu, A.M. Abduljalil, A. Kangarlu and P.M. Robitaille, High signal-to-noise FLASH imaging at 8 Tesla, Magn Reson Imaging, 17(8):1099-1103, 1999.
8. Y. Zhu, Acceleration of focused excitation with a transmit coil array, Proceedings of the ISMRM 10th Scientific Meeting, p 190, 2002.
9. U. Katscher, P. Börnert, C. Leussler and J. van den Brink, Theory and experimental verification of transmit SENSE, Proceedings of the ISMRM 10th Scientific Meeting, p 189, 2002.
10. U. Katscher, P. Börnert, C. Leussler and J.S. van den Brink, Transmit SENSE, Magn Reson Med, 49:144-150, 2003.
11. Y. Zhu, Parallel excitation with an array of transmit coils, Magnetic Resonance in Medicine, 51:775-784, 2004.
12. Y. Zhu, RF power reduction with parallel excitation, Proceedings of the ISMRM 12th Scientific Meeting, p 331, 2004.
13. P.B. Roemer, W.A. Edelstein, C.E. Hayes, S.P. Souza and O.M. Mueller, The NMR phased array, Magn Reson Med, 16:192-225, 1990.
14. K.P. Pruessmann, M. Weiger, M.B. Scheidegger and P. Boesiger, SENSE: sensitivity encoding for fast MRI, Magn Reson Med, 42:952-962, 1999.
15. D.K. Sodickson and W.J. Manning, Simultaneous acquisition of spatial harmonics (SMASH): ultra-fast imaging with radiofrequency coil arrays, Magn Reson Med, 38:591-603, 1997.
16. C.E. Hayes, W.A. Edelstein, J.F. Schenck, O.M. Mueller and M. Eash, An efficient, highly homogeneous radiofrequency coil for whole-body NMR imaging at 1.5T, J Magn Reson, 63:622-628, 1985.
17. J.T. Vaughan, H.P. Hetherington, J.O. Otu, J.W. Pan, G.M. Pohost, High frequency volume coils for clinical NMR imaging and spectroscopy, Magn Reson Med, 32:206-218, 1994.
18. Y. Zhu and R. Giaquinto, Improving flip angle uniformity with parallel excitation, Proc. of the 13th meeting of the International Society for Magnetic Resonance in Medicine, p 2752, May 05, Miami Beach.
19. J. Pauly, D. Nishimura and A. Macovski, A linear class of large-tip-angle selective excitation pulses, J Magn Reson, 82:571-587, 1989.
20. Y. Zhu, RF power deposition and 'g-factor' in parallel transmit, Proceedings of the 14th meeting of the International Society for Magnetic Resonance in Medicine, May 06, Seattle. (submitted)

21. Röschmann, Imaging of dielectric resonance mode patterns with a 4T whole body MR system, Proceedings of the 7th SMRM, p 267, 1988.
22. Tropp J, Image brightening in samples of high dielectric constant, J Magn Reson, 167:12-24, 2004.
23. C. Gabriel, S. Gabriel and E. Corthout, The dielectric properties of biological tissues, Phys. Med Biol, 41:2231-2249, 1996.
24. H. Vesselle and R.E. Collin, The signal-to-noise ratio of nuclear magnetic resonance surface coils and application to a lossy dieletric cylinder model – Part II: the case of cylindrical window coils, IEEE Trans Biomed Eng, 42:507-520, 1995.
25. Proceedings of the 13th meeting of the International Society for Magnetic Resonance in Medicine, May 05, Miami Beach.
26. Y. Zhu, R. Watkins, R. Giaquinto, C. Hardy, G. Kenwood, S. Mathias, T. Valent, M. Denzin, J. Hopkins, W. Peterson and B. Mock, Parallel excitation on an eight transmit-channel MRI system, Proceedings of the 13th meeting of the International Society for Magnetic Resonance in Medicine, p 14, May 05, Miami Beach.
27. P. Ullmann, S. Junge, M. Wick, W. Ruhm and J. Hennig, Experimental verification of transmit SENSE with simultaneous RF-transmission on multiple channels, Proceedings of the 13th meeting of the International Society for Magnetic Resonance in Medicine, p 15, May 05, Miami Beach.